

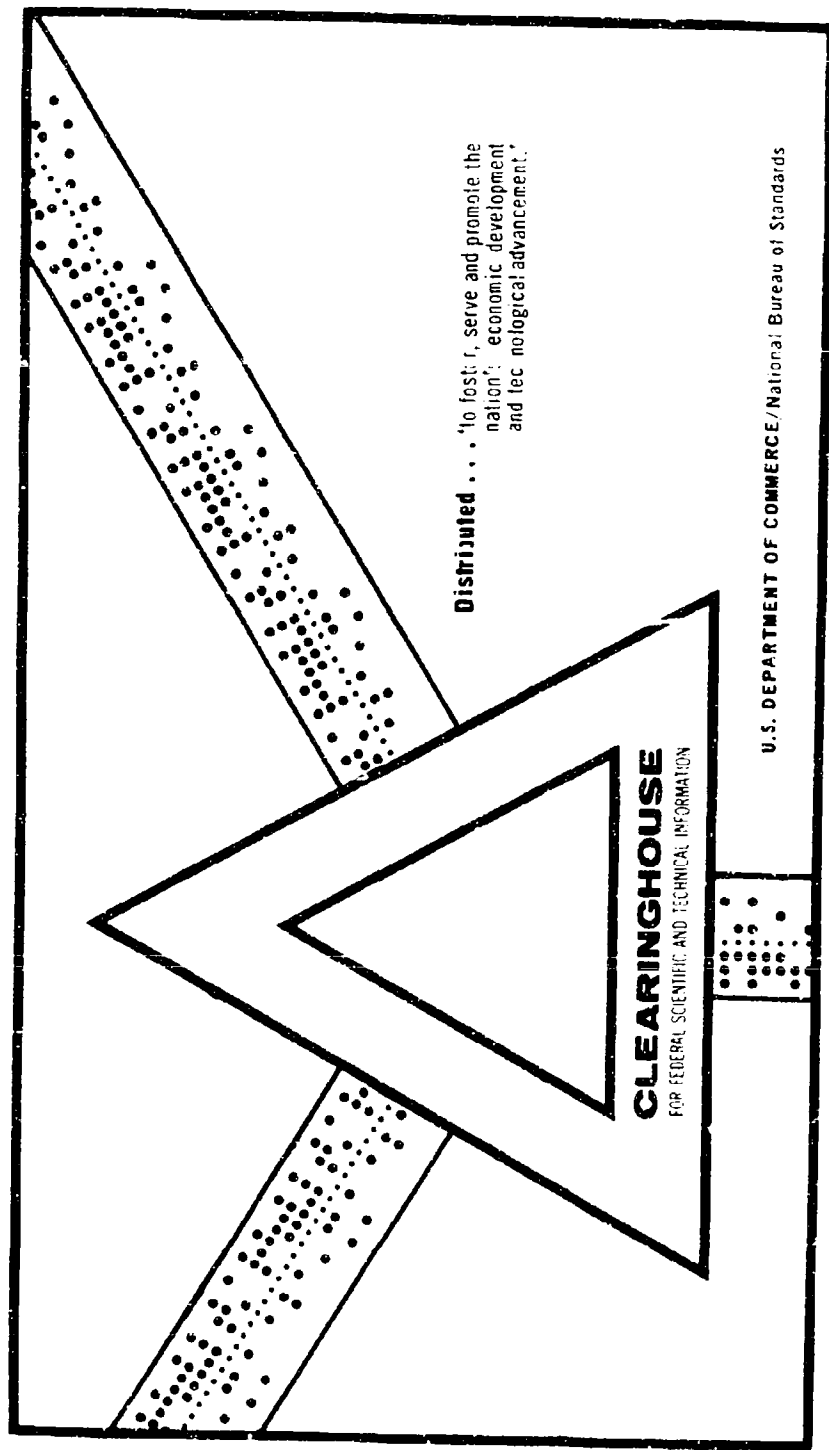
AD 696 292

ELF PROPAGATION AND EMISSION IN THE MAGNETOSPHERE

H. B. Liemohn

Boeing Scientific Research Laboratories
Seattle, Washington

October 1969



This document has been approved for public release and sale.

SCIENTIFIC RESEARCH LABORATORIES

AD696292

ELF Propagation and Emission in the Magnetosphere

H. B. Liemohn

This document has been approved
for public release and sale; its
distribution is unlimited.

GEO-ASTROPHYSICS LABORATORY

NOV 14 1969

AUGUST 1969

61

D1-82-0890

ELF PROPAGATION AND EMISSION
IN THE MAGNETOSPHERE

by

H. B. Liemohn

Geo-Astrophysics Laboratory
Boeing Scientific Research Laboratories
Seattle, Washington 98124

August 1969

Revised October 1969

Presented at the International Union of Radio Science
(URSI) XVIth General Assembly in Ottawa, Canada,
18-28 August 1969. To be published in the Proceedings
of the Assembly.

ELF PROPAGATION AND EMISSION IN THE MAGNETOSPHERE

by

H. B. Liemohn

ABSTRACT

Considerable research progress has been achieved on ELF signals in the magnetosphere as a consequence of satellite and ground-based studies. Attention will be focused on the frequency band from 0.2 to 500 Hz, which is well below the minimum electron plasma and cyclotron frequencies, so that the hydromagnetic approximation applies. Although the magneto-ionic medium is anisotropic and inhomogeneous, the propagation theory for the fast and Alfvén modes in homogeneous media is adequate at these frequencies. The signal velocity of the fast mode is essentially isotropic for frequencies below the lower hybrid resonance. The Alfvén mode is restricted to frequencies below the proton cyclotron frequency and its signal velocity is closely guided by the geomagnetic field. The polarization of the modes is nominally right and left for the fast and Alfvén, respectively, and circular only for propagation parallel to the field.

The morphology of these modes in remote regions of the magnetosphere is being developed from satellite studies. Statistics are available now on the ELF noise distributions with latitude, local time, and geomagnetic activity. Triaxial search coil magnetometers have measured wave polarization and found it to be predominantly right handed above the local proton cyclotron frequency. The noise power spectrum near the magnetosheath is similar to that observed on the ground. During magnetospheric substorms the noise level increases as anticipated.

Studies based on ground observations have concentrated on dispersion, polarization, and amplitude analyses. Due to ionospheric attenuation, ground observations of ELF signals from the magnetosphere are limited to frequencies below about 10 Hz. In the band from 0.2 to 10 Hz, however, many types of geomagnetic micropulsation signals are observed. The characteristic dispersion of one class of signals led to its interpretation as Alfvén-mode waves which propagate back and forth along field-line paths. These "ULF whistlers" are sufficiently well documented to permit their use as magnetospheric probes of the thermal plasma distribution. Polarization studies have attempted to isolate the propagation modes, but coupling in the ionosphere has hampered progress. Signal amplification by the cyclotron-resonance interaction with energetic particles, and attenuation in the ionospheric waveguide have been extensively investigated theoretically.

Several recommendations concerning future research may be offered. Foremost among them is the necessity for more cooperative programs between research groups due to the global nature of the phenomena. To this end, up-to-date tabulations of ground stations and satellites have been prepared, and more emphasis could be placed on "regular geophysical days." Calibrated amplitude spectra are needed in view of their potential as remote sensing parameters. Similarly polarization properties are vital to the interpretation of signals. Finally, the establishment of remote ground stations in uninhabited locations should be considered.

TABLE OF CONTENTS

	Page
INTRODUCTION	1
PROPAGATION THEORY	3
SATELLITE STUDIES	11
GROUND STUDIES	14
FUTURE RESEARCH	26
APPENDIX	29
REFERENCES	44

FIGURE CAPTIONS

	Page
Fig. 1. Schematic diagram of hydromagnetic wave propagation modes at frequencies well below the ion-cyclotron frequency.	4
Fig. 2. Cyclotron-resonance amplification of hydromagnetic wave packets propagating along field-line paths for specific energy (E) and pitch angle (α) distributions of ions (34).	9
Fig. 3. Ampligram display of a typical ULF whistler event (91, 92)	16
Fig. 4. Plasmopause dynamics observed by OGO 3 and ULF whistler dispersion analysis (85,86).	20
Fig. 5. Detailed amplitude measurements of the eight elements of the ULF whistler event shown in Fig. 3 (91).	23
Fig. 6. Global distribution of rapid-run geomagnetic observatories. Geomagnetic coordinates, based on the Jensen and Cain model (107 & 107a), are field-line L-shells and longitude lines spaced at hour intervals.	39

INTRODUCTION

The purpose of this paper is to succinctly summarize current research on extremely low frequency (ELF) propagation and emission in the magnetosphere. The topic is restricted to satellite research in the frequency band from 0.2 to 500 Hz and ground-based research in the band from 0.2 to 10 Hz. ELF signals are observed primarily as rapid variations in the geomagnetic field using various magnetometers. A wide range of signal characteristics are encountered depending on the modes of propagation, source mechanisms, and local conditions along the propagation path. These properties permit the signals to be used as remote sensors of several important magnetospheric parameters which is the motivation for this research.

Several comprehensive reviews of ground-based research in this field have appeared in recent years (1-8). The reader who wants to pursue some aspect of this subject in depth is directed to these detailed compendia as well as the original literature. More recent satellite results at these frequencies have not been formally reviewed, but excellent summaries of the scientific results from magnetometer experiments in the OGO series are now available (9,10).

A large amount of very good research has been performed in the field of ELF propagation, as evidenced by the long reference lists in review papers. In an effort to make this summary more readable, the references to recent original literature have been collected at the beginning of each short subsection. No attempt will be made to cite individual research results as is customary in comprehensive reviews. The subsections of this paper are collected under four main sections: propagation theory, satellite studies, ground studies, and future research.

PROPAGATION THEORY

Hydromagnetic approximation. The propagation of ELF signals in the magnetosphere is usually described by the hydromagnetic approximation in which the inertial effects of the electrons are ignored, since the frequencies of interest are well below the electron plasma and cyclotron frequencies Π_e and Ω_e . In general there are three modes of propagation in a magnetionic medium, namely, two electromagnetic waves with transverse fields and an acoustic wave. In this approximation the mode that is polarized in the left-hand sense is called the "Alfvén" mode, the mode with right-hand polarization is called the "fast" mode, and the acoustic mode is called the "slow" mode. The mathematical description of these modes varies considerably depending on the assumptions about the medium.

The simplest description is obtained for propagation in a homogeneous cold plasma when the frequencies are well below the ion plasma and cyclotron frequencies, Π_i and Ω_i . The modes in the well-known case (11, 12), in which the medium is treated like a compressible, conducting fluid, are shown schematically in Figure 1. The phase velocity surfaces depend

Hydromagnetic Propagation Modes

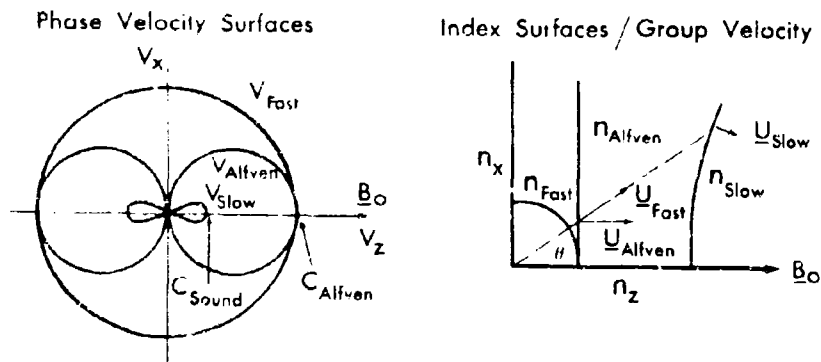


Fig. 1. Schematic diagram of hydromagnetic wave propagation modes at frequencies well below the ion-cyclotron frequency.

chiefly on the Alfvén speed $V_A = B_0 / (4\pi\rho_0)^{1/2}$ and the sound speed $V_S = (\gamma p_0 / \rho_0)^{1/2}$ where B_0 is the static field, ρ_0 is the ion-mass density, p_0 is the static gas pressure and γ is the ratio of specific heats. For quantities appropriate to the magnetosphere, $V_A \gg V_S$ so that the slow mode may be ignored in most applications. The mode characteristics shown in Figure 1 are typical of ELF propagation in the lower magnetosphere and ionosphere. Although the medium is anisotropic, the signal velocity of the fast mode is essentially isotropic whereas the signal velocity of the Alfvén mode is closely guided by the magnetic field.

In remote regions of the magnetosphere, near its boundary and in the tail, the frequencies of interest are close to both Ω_1 and Ω_i which require more elaborate formulation (13-16) of the cold plasma approximation. In this parameter regime the wave normal surfaces and group velocity surfaces are distorted considerably from the simple case. The Alfvén mode is restricted to frequencies below Ω_1 where it has a resonance, and its group velocity remains closely guided along the field. The fast mode remains unrestricted up to the lower hybrid resonance frequency ω_{LHR} , where a cone of forbidden wave normals is encountered perpendicular to the

static field. However, fast mode signals continue to propagate at large angles to the field at frequencies up to Ω_e .

Applications. Certain aspects of hydromagnetic propagation in the magnetosphere and ionosphere have received special attention. In the magnetosphere, field-line guidance of Alfvén waves has been investigated (17-19) to ascertain the effects of inhomogeneity. Ray path calculations in a realistic geomagnetic field have shown that the field curvature does not appreciably diverge the signal away from the field. Guidance by field-aligned ducts of enhanced or depressed ionization is also feasible but apparently not essential.

Propagation in and through the ionosphere has been a particularly vexing problem due to the complications of mode coupling and guiding as well as the usual transmission, reflection, and absorption processes. Absorption of hydromagnetic energy is known to increase rapidly with frequency producing an upper limit near 10 Hz in ground observations. Just below this cutoff, the ionosphere remains relatively opaque to direct wave penetration, and instead the hydromagnetic energy is confined to a waveguide shell between 100 and 1000 km from which it leaks to the ground. Since ionospheric quantities

have steep gradients, a full-wave treatment with its attendant numerical methods is mandatory.

Refinements in the attenuation theory have produced more realistic estimates (20-23) of direct transmission properties. There is a large diurnal variation with maximum absorption during the daytime. However, ionospheric heating by ELF waves is negligible compared to other sources except possibly during geomagnetic storms. The physics of the ionospheric waveguide has been developed extensively as well (24-28). In the waveguide the fast mode has a group velocity of around 600 km/s and is strongly attenuated during the day. Enhanced attenuation below 0.5 Hz effectively band limits the mode for long distance transmission. Coupling between the Alfvén and fast modes is sharply peaked in the lower F-region permitting large amounts of Alfvén wave energy from the magnetosphere to enter the waveguide. However, realistic estimates of the net reflection and transmission of energy by the ionosphere remain uncertain due to the large number of independent parameters.

Wave-Particle Interactions. Research on hot plasma effects at these frequencies has centered on the cyclotron-resonance interaction. Due to motion parallel to the static field, particles encounter a Doppler shifted wave frequency. When

this frequency equals the cyclotron frequency of the particle and the wave polarization as seen by the particle has the same sense as the particle gyration, the resonance takes place. Evidently both Alfvén and fast mode waves may interact with either protons or electrons. In practice the dominant interaction is between Alfvén waves and nonthermal protons (above 100 eV). The net amplification or attenuation of the waves depends critically on the shape of the particle distribution as well as the frequencies.

The cyclotron instability of particle streams in thermal background plasma has been suggested (29-31) as a source of hydromagnetic energy, but their generation and maintenance is unlikely. When the nonthermal proton distribution in the steady-state quiescent magnetosphere is sufficiently anisotropic, however, Alfvén mode waves may be strongly amplified (32-41). Examples of the power transfer for interhemisphere field-line paths are shown in Figure 2 for energy and pitch angle distributions of the form $E^{-n} \sin^m \alpha$. The waves are subject to Landau damping when their propagation vector is not parallel to the static field, but cyclotron resonance amplification still dominates if the energy distribution is sufficiently hard.

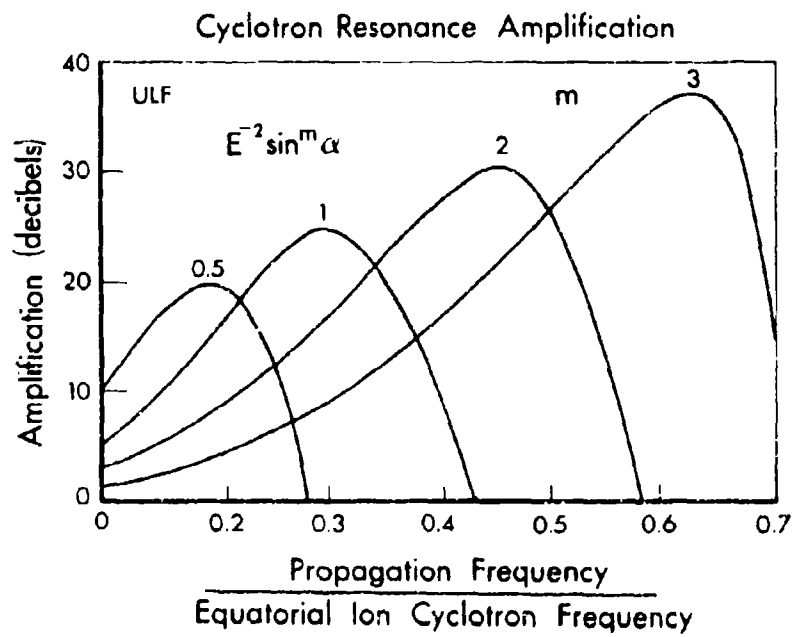


Fig. 2. Cyclotron-resonance amplification of hydro-magnetic wave packets propagating along field-line paths for specific energy (E) and pitch angle (α) distributions of ions (34).

Since the cyclotron resonance occurs over a broad range of particle energies, the interaction is capable of redistributing energy and modifying pitch angles (42-47). Using quasi-linear theory, the equilibrium configuration of waves and particles in the magnetosphere has been realistically estimated, but the complete nonlinear theory remains to be developed. The effects of the interaction have been evaluated statistically as well to ascertain diffusion rates parallel and orthogonal to the field. Cyclotron damping of magnetosonic waves may also heat the magnetospheric plasma differentially, accounting for the excess energy in the proton distribution in the neutral sheet of the tail.

Other mechanisms involving ELF waves also affect the wave-particle equilibrium in the magnetosphere (48-50). Random scattering by hydromagnetic wave fields may be characterized by a net diffusion coefficient in pitch angle. In addition the mirror geometry of the geomagnetic field allows resonant pitch-angle scattering at the bounce frequency of the particles.

SATELLITE STUDIES

Magnetosphere boundary. Several spacecraft carrying magnetometers with ELF sensitivity have traversed the boundary region of the magnetospheric cavity (51-57). The location of the magnetopause and shock surfaces which bound the magnetosheath are easily identified in satellite data so that the morphology of the accompanying wave structure can be isolated. In the shock transition region both random incoherent noise and discrete coherent signals are found over the band from 0.1 to 500 Hz. Above 10 Hz the power spectral density falls approximately as $(\text{frequency})^{-3}$ and tends to flatten off below. The signals are detected both upstream on the solar wind side and downstream in the magnetosheath. The total energy density of these wave fields is less than 1% of the average solar wind kinetic energy density.

Since the amplitude of the signals decreases by one to two orders of magnitude away from the shock front, it is fair to assume that their source is in the shock mechanism. Below 10 Hz the discrete signals are contained in wave packets of only a few cycles with amplitudes as high as a gamma. Above 10 Hz

nearly monochromatic wave packets occur at random frequencies with amplitudes from 10 to 100 milligamma. Since these high frequency signals last several seconds in the magnetosheath, some amplification mechanism is suggested. The transverse polarization of these signals is approximately circular which suggests propagation in the fast and Alfvén modes.

Although insufficient parameters are available at this time to identify the modes, some speculation is feasible on the basis of what is known. The ambient magnetic field is about 30 gamma which gives $\Omega_i \sim 0.5$ Hz, $\omega_{LHR} \sim 20$ Hz and $\Omega_e \sim 900$ Hz. There is evidence in the power spectra of the waves for changes of slope near 1 Hz and 30-100 Hz which may be attributed to the disappearance of the Alfvén mode above Ω_i and reduced fast mode propagation above ω_{LHR} . In addition the relatively large amplitude of some signals near Ω_i is suggestive of wave-particle interactions which could amplify the signals.

Magnetosphere. Measurements of ELF (below 500 Hz) within the magnetosphere have not been analyzed extensively until quite recently (58,59). Inside the magnetopause there is a sharp decrease in wave energy density throughout the ELF band. Evidently very little shock wave energy penetrates this boundary

directly, and consequently a different source mechanism must account for the hydromagnetic energy inside the magnetosphere. Again the signals consist of both bursts and steady noise, but the predominant frequency regime is somewhat higher and the amplitude is lower than that in the boundary region.

The steady ELF noise about 10 Hz is generated principally on the dayside of the magnetosphere over the latitude region 10° to 50° on L-shells from 6 to 10 although strong signals are detected as low as $L = 2$. The source of this energy is probably a plasma instability at Ω_i caused by a pitch angle anisotropy of the trapped particles. The frequency range and power of these waves seems to be sufficient to account for the steady electron precipitation in the energy range from 20 to 200 keV. Observations of ELF noise at the base of the magnetosphere are consistent with observations in the source region, but low altitude data alone provides an incomplete picture of ELF throughout the magnetosphere.

Bursts of ELF noise are found principally within 20° of the equator at L-shells beyond 5. There is a strong day-night asymmetry with most probable occurrence between 0400 and 1800 local time. This source region is consistent with the region where auroral microbursts of electrons and VLF chorus are found. This close association with related geomagnetic activity is evidently another manifestation of wave-particle interactions.

A different group of ELF signals has been discovered in the immediate vicinity of the equator just inside the plasmapause. The noise consists of a broad enhancement between $2\Omega_i$ and ω_{LHR} with numerous discrete peaks. Incredible though it may seem these signals are only detected within 2° of the equator and propagate nearly perpendicular to the static field. Only the fast mode can satisfy these criteria. The amplitude of this noise is about 10 milligamma which is sufficient to produce the observed pitch angle diffusion of electrons mirroring near the equator.

GROUND STUDIES

Pc 1 Morphology. Our knowledge about the properties of continuous geomagnetic-pulsation trains in the ELF frequency band from 0.2 to 10 Hz (Pc 1 class) has continued to grow from ground station observations. Many types of signal noise are observed in the Pc 1 category, but one unusual type has been singled out for extensive study due to its measurable structure. This section is concerned only with the morphology of these signals leaving discussions of dispersion, polarization, and amplification to later subsections.

The type of Pc 1 events under study consist of a series of rising tones over a narrow bandwidth that repeat at regular intervals which is illustrated in Fig. 3. The event is interpreted (60, 61) as an Alfvén mode wave packet that propagates back and forth along a field-line path producing multihop echoes at the ground station. The spacing of 2 to 4 minutes between elements is indicative of a group velocity around 300 km/s along the path. Frequently the events occur in complicated overlapping clusters of events which may last for several hours. The characteristic ascending tone is attributed to the frequency-time dispersion inherent in the mode. At the base of the path, the energy scatters into the ionosphere waveguide and subsequently leaks to the ground over a broad area. On the ground the signal amplitudes are normally a few tens of milligammas so that their amplitude in the magnetosphere must be close to a gamma. Although the explanation for these events seems well established, their impulsive source has not been determined. In the course of research these events have been called pearls, hydromagnetic emissions, screamers, micropulsation whistlers, hydromagnetic whistlers, and ULF whistlers, and their nomenclature remains unsettled at this time. For purposes of identification the name ULF whistlers will be used here.

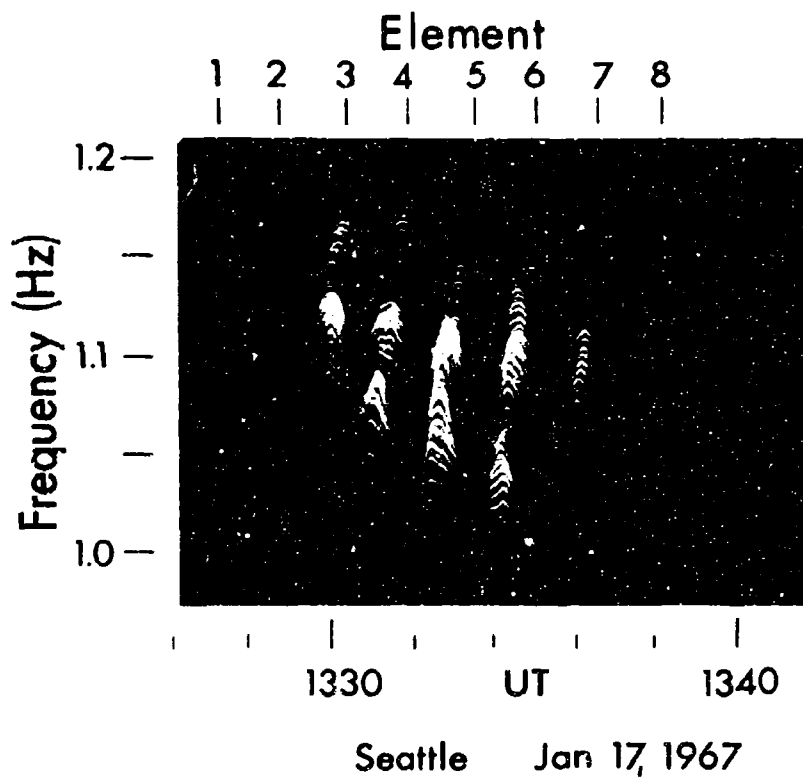


Fig. 3. Ampligram display of a typical ULF whistler event (91, 92).

One phase of research on these signals has concentrated on general patterns of frequency, occurrence, and conjugacy (62-71). On the basis of ground observations at several locations, the propagation frequency was recognized as a significant measure of the path location. Empirically it was found that frequencies from 0.3 to 3 Hz corresponded to L-shell paths from 10 to 4 respectively. The occurrence of ULF whistlers varies with latitude, and a diurnal pattern has been established that is similar to the auroral oval, that is, lower invariant latitude at night than day. The appearance of the wave packet in alternate hemispheres is not exactly 180° out of phase, but discrepancies are attributed to differences of travel time in the ionospheric waveguide. Ionospheric attenuation has been estimated experimentally by comparing simultaneous events at conjugate stations where the ionosphere above one was never sunlit; the amplitude ratios decreased during the daytime and also with increasing frequency in agreement with theoretical predictions.

Correlations between ULF whistlers and other types of geophysical phenomena have also received considerable attention (72-76). Special significance must be accorded the fact that these events occur principally during the calm period 3 to 7 days after a geomagnetic storm. It is not clear whether source, propagation, or

amplification conditions are responsible for this circumstance, but evidently the temporary state of magnetospheric relaxation is vital. A positive correlation with magnetospheric substorms is in doubt, although some ULF whistlers have been observed during these periods of activity. Other types of geomagnetic micropulsations do appear to be well correlated with substorms. Over the eleven-year solar cycle, the occurrence of these signals peaks sharply around the inflection points intermediate between solar-cycle extrema, which indicates a complicated secondary dependence on geomagnetic storm physics.

ULF Whistler Dispersion. Nearly all measurable events exhibit a small dispersion between successive elements which is attributed to the frequency dependence of the Alfvén group velocity. Since the group velocity depends on the geomagnetic field and the thermal plasma density along the propagation path, the dispersion measurements have provided a means for remotely probing the magnetosphere. Large collections of data have been analyzed (77-86) to estimate the density distribution.

The propagation paths are confined to L-shells between 4 and 10 and their diurnal distribution confirmed the previous empirical estimate. The frequencies of the ULF whistlers are limited

between 0.2 and 0.7 R_1 (equatorial) and their bandwidths vary from 0.1 to 0.3 R_1 (equatorial). The "best fit" density distribution obtained from the data falls off more rapidly than the well-known hydrostatic equilibrium but less rapidly than the plasmopause. This apparent disagreement with the results from VLF whistler analysis may be resolved by recalling that most ULF whistlers are detected only during the recovery phase of geomagnetic storms. At this time the plasmopause is not so sharply defined and is moving outward as shown in Fig. 4, so that ULF whistlers are probably a measure of this dynamic process. The presence of helium ions along the path would distort the dispersion pattern into a nose, but this type of event is rarely detected.

ULF Whistler Polarization. Studies of the signal polarization (26, 87-90) have revealed some unusual and puzzling results. According to the hydromagnetic wave theory, the polarization of Alfvén mode signals is left-handed with respect to the magnetic field direction. However ground observations have found it consists of a mixture of random, linear, right, and left-hand polarizations. This might have been anticipated from the complicated transmission in and through the ionosphere. Indeed, recent theoretical analysis has shown that ionospheric mode coupling is subject to several conditions which scramble the wave sense. The left-hand sense is expected to dominate at night, at higher frequencies, and at polar latitudes,

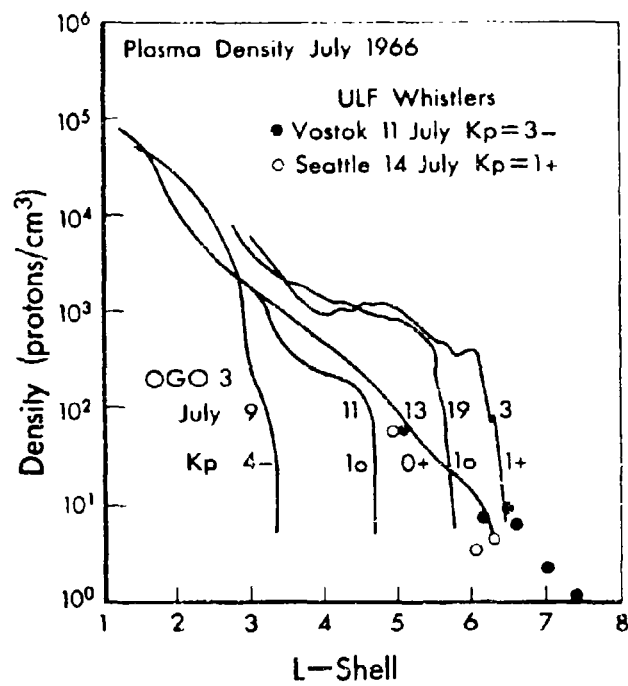


Fig. 4. Plasmapause dynamics observed by OGO-3 and ULF whistler dispersion analysis (85, 86).

which seems to fit some experimental findings. However, observations at conjugate stations have revealed that occasionally the polarization is identical and changes rapidly at both locations suggesting a magnetospheric property.

One aspect of the experimental technique deserves special comment since natural signals are not always ideally suited for polarization measurements. It is important to use only isolated events and narrow band filters to avoid contamination by overlapping signals. Due to phasing of overlapping Fourier components it is quite possible to obtain spurious results if each wave packet element is not well isolated from its neighbors. Narrow band filters also introduce spurious phasing effects which must be accounted for.

Cyclotron-resonance amplification. The long lifetime of wave packets which produce ULF whistlers requires amplification of the signals. The amplitude of successive elements frequently grows for several echoes before decaying slowly away. Furthermore, the complex mode coupling and attenuation in the ionospheric waveguide imposes severe losses at the ends of the path which must be overcome for repetition of the signal. A strong candidate for the source of the signal energy is the cyclotron

resonance interaction with energetic particles along the magnetospheric path. Details of the mechanism are given in the section on propagation theory; only its application to individual ULF whistlers is described here (34, 37, 39, 91, 92).

An example of typical magnetospheric amplification which might be encountered during quiescent times is shown in Fig. 2. Evidently potential bands of amplification are in reasonable agreement with observed propagation bands. The shape and band limits of the theoretical curves depend on the shape of the phase space distribution of energetic particles, and the magnitude depends on the number of particles. If the mechanism is verified, measurements of amplification between successive echoes may become a vital ground-based probe of energetic particle distributions. The fact that ULF whistlers are usually detected only after geomagnetic storms may be attributed to lack of appreciable amplification except during this period.

Both digital and analog methods are currently available for the measurement of successive amplitudes of ULF whistler echoes. Fig. 5 illustrates the detailed growth and decay of the event shown in Fig. 3. When successive echoes are compared, the effects of ionospheric transmission cancel out and only the ionospheric

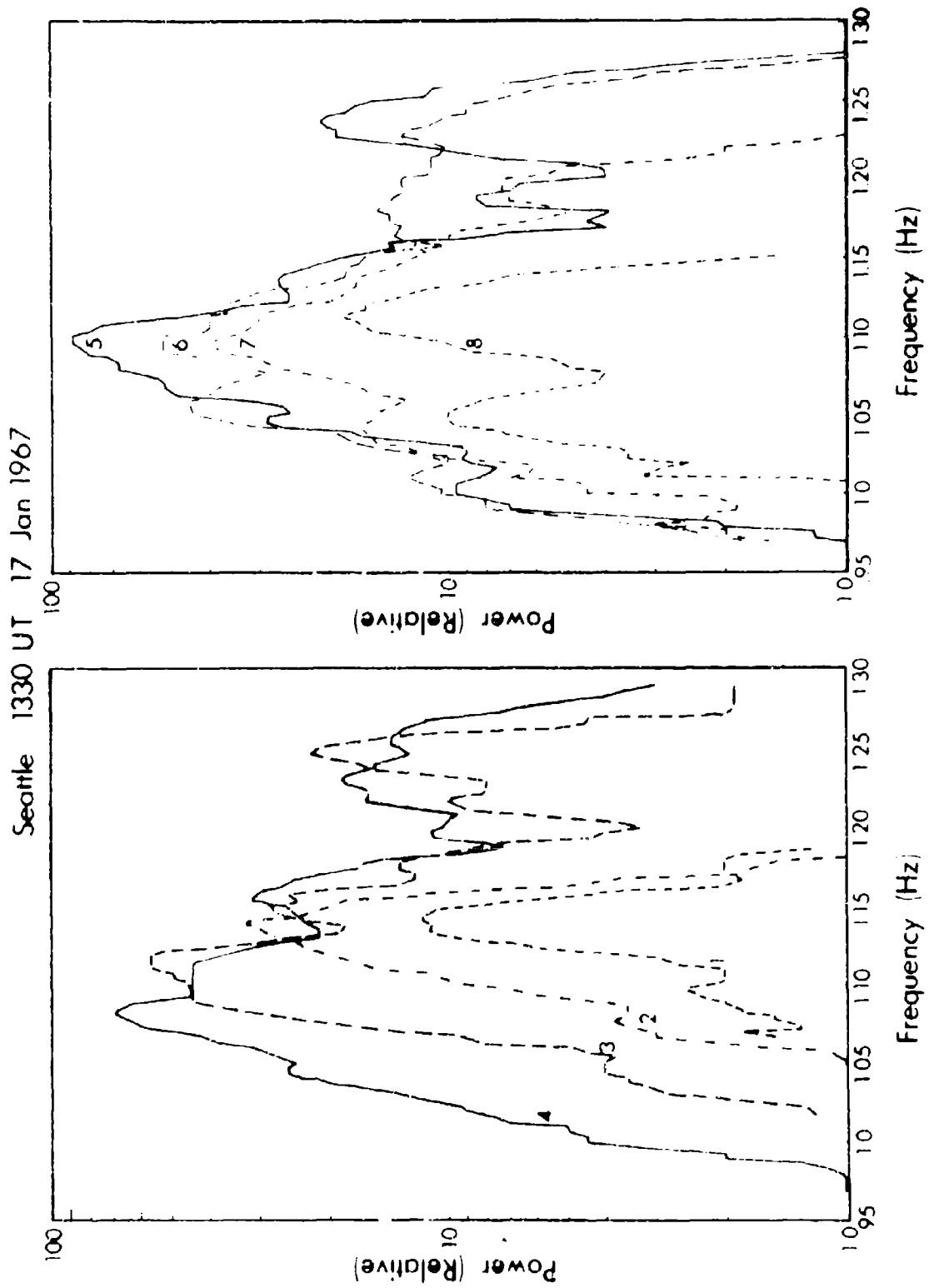


Fig. 5. Detailed amplitude measurements of the eight elements of the ULF whistler event shown in Fig. 3 (91).

planning of joint ground-satellite observations, programs are underway to predict the geomagnetic field-line projection of satellite orbits. Advance notice of opportunities is essential for good coverage of field-aligned phenomena.

The existing permanent network of stations should be supplemented by several portable units that could extend local latitude and longitude chains as well as improve global coverage. The rate at which analog data is reduced to a usable form would be improved substantially by time sharing of new multichannel, ultrafast, frequency-amplitude analyzers. Remote ground stations which record digitally might be interrogated continuously in real time using satellite transponders.

The analysis of ELF signal data on the basis of frequency-time dispersion is well established as a tool of the trade. However, signal amplitude and polarization are also key parameters for understanding the physical processes of the magnetosphere. Amplitude relates directly to wave-particle interactions and polarization is vital for proper mode identification. Physical parameters and indices which characterize known ELF signals should be developed in order to provide a means for routine analysis. Such digested quantities form a useful basis for the evaluation of new theoretical and experimental research and should be collected by the world data center on a variety of geophysical phenomena.

APPENDIX

In order to facilitate joint cooperative research programs between groups of ground observers and ground-satellite observers, lists of rapid-run magnetometer experiments at ground stations and in spacecraft have been prepared. Table 1 contains ground stations, their coordinates, their frequency range according to the Pc classification (1, 0.2-5s; 2, 5-10s; 3, 10-45s, 4, 45-150s; 5, 150-600s), and data analysts. The geomagnetic coordinates in this table are based (106a) on a north geomagnetic pole at 78.5 N and 291.0 E geographic (longitude is measured eastward from the 291.0 E geographic meridian). Names listed as analysts have published results based on the data recorded at that station and are not necessarily the personnel responsible for its operation. The global distribution of ground stations is shown in Fig. 6. Table 2 contains spacecraft experiments, their orbits, types of instruments, and experimenters.

Preparation of these tables required the assistance of many individuals which the author gratefully acknowledges. Previously published tabulations (102, 106) provided an initial basis on which to build. These were updated by Mrs. H. B. Knafllich of BSRL who made an extensive search of the open literature. Many researchers have contributed revisions and corrections to an early draft that was distributed. Undoubtedly errors and omissions are still present and the author invites interested persons to offer improvements.

TABLE 1. RAPID-RUN GEOMAGNETIC MICROPULSATION OBSERVATORIES

OBSERVATORY	COUNTRY	SPONSOR	POSITION COORDINATES		Pc FREQ. BAND	ANALYST
			GEOGRAPHIC	GEOMAGNETIC		
			LAT.	LONG.	LAT.	LONG.
Makere	Uganda	U.K.	00.5 N	32.5 E	12.6 S	2-5 David Orr-UK
Legon	Ghana	U.K.	05.63 N	00.18 W	03.0 S	2-4 V.R.S. Hutton-UK
*Bangui	Cent.-Afr. Rep.	France	04.43 N	18.57 E	04.8 N	88.5 1-5 O. Fambitakoye-Fr
Landa (Ft. Archambault)	Chad	France	09.16 N	18.36 E		1-5 J. Roquet-Fr
Ibadan	Nigeria	U.K.	07.43 N	03.9 E	10.7 N	74.6 A. Onwumechilli-Ni
*M'Bour	Senegal	France	14.4 N	16.95 W	21.5 N	55.1 1-5 H.G. Barszus-Fr
Freetown	Sierra Leone	Sierra Leone	08.47 N	13.22 W	14.8 N	57.8 4 { D.G. Osborne D. Rivers
*Addis Ababa	Ethiopia	Ethiopia	09.03 N	38.77 E	05.4 N	109.2 1-5 J. Roquet-Fr
Parakou	Dahomey	France	09.35 N	02.62 E	12.6 N	74.8 1-5 " 30
*Hermanus	R.S. Africa	R.S. Africa	34.42 S	19.23 E	33.7 S	80.7 { A.M. van Wijk-RSA R. Schlich-vr
Tamanrasset	Algeria	Algeria	22.8 N	05.52 E	25.07 N	80.1 1-5 M. Kacimi
*Moca	Fernando Poo Is.	Spain	03.35 N	08.67 E	05.7 N	78.6
Ashkhabad	USSR	USSR	37.95 N	58.10 E	30.5 N	133.1 1-5 V.A. Troitskaya-USSR
Alma-Ata	USSR	USSR	43.25 N	76.92 E	33.4 N	150.7 1-5 { S.V. Bortakov-USSR
Borok	USSR	USSR	58.03 N	38.97 E	53.0 N	123.2 1-5 " 1-5
Petropavlovsk	USSR	USSR	53.1 N	158.63 E	44.7 N	218.2 1-5 " 1-5
Lovozero	USSR	USSR	67.98 N	35.08 E	62.9 N	127.0 1-5 " 1-5
Sogra	USSR	USSR	62.8 N	46.25 E	57. N	128. 1-5 " 1-5
Irkutsk	USSR	USSR	52.47 N	104.03 E	41. N	174.4 1-5 " 1-5
Stepanovka (Odessa)	USSR	USSR	46.78 N	30.9 E	43.8 N	111.1 1-5 " 1-5
Kiev	USSR	USSR	50.72 N	30.30 E	47.6 N	112.2

* Standard observatories producing normal magnetograms.

OBSERVATORY	COUNTRY	SPONSOR	POSITION COORDINATES				Pc FREQ. BAND	ANALYST
			GEOGRAPHIC		GEOMAGNETIC			
			LAT.	LONG.	LAT.	LONG.		
Yakutsk	USSR	USSR	62.02 N	129.67 E	51.0 N	193.8	1-5	V.A. Troitskaya-USSR
Cape Wollen	USSR	USSR	66.17 N	169.83 W	61.8 N	237.1	1-5	S.V. Burtakov-USSR
Tixie	USSR	USSR	71.58 N	129. E	60.4 N	191.4	1-5	"
Cape Chelyuskin	USSR	USSR	77.72 N	104.28 E	65.9 N	177.5	1-5	"
Dixon Island	USSR	USSR	73.53 N	80.55 E	63.0 N	161.4	1-5	"
Tikhaya Bay (Heiss Is.)	USSR	USSR	80.62 N	58.05 E	71.3 N	155.3	1-5	"
Thilisi	USSR	USSR	42.08 N	44.70 E	36.7 N	122.1		
Ulan Bator	Mongolia	Mongolia	47.85 N	106.75 E	36.4 N	176.5	2-5	G. Dodon-USSR
Dunedin	New Zealand	New Zealand	46. S	171. W	51. S		1-3	R.L. Dowden
Oamaru	New Zealand	New Zealand	44.99 S	170.97 E	47.7 S	250.	1-5	E.M. Wescott-US
Invercargill	New Zealand	New Zealand	47.2 S	168.3 E			1-5	J.R. Storey M.J. Polletti
Auckland	New Zealand	New Zealand	36.51 S	174.45 E	42.7 S	253.6	1-5	J.R. Storey
Port Moresby	New Guinea	Australia	9.40 S	147.15 E	18.6 S	217.9	1-5	
Lae	New Guinea	Australia	6.07 S	146.9 E			1-5	J.S. Mainstone-Aus R.W.E. McNicol
U. of Newcastle NSW	Australia	Australia	32.75 S	151.5 E	42.0 S	226.	1-5	B.J. Fraser-Aus
Esk (Brisbane)	Australia	Australia	27.25 S	152.50 E	35.8 S	226.9	1-5	J.S. Mainstone-Aus R.W.E. McNicol
Toolangi (Melbourne)	Australia	Australia	37.53 S	145.47 E	46.7 S	220.8	1-5	"
Hobart, Tasmania	Australia	Australia	42.87 S	147.33 E	52.0 S	223.	1-5	B.J. Fraser J.S. Mainstone

OBSERVATORY	COUNTRY	SPONSOR	POSITION COORDINATES			Pc FREQ. BAND	ANALYST
			GEOGRAPHIC LAT.	LONG.	GEOMAGNETIC LAT.	LONG.	
Townsville, Qld.	Australia	Australia	19.32 S	146.73 E	29.0 S	217.	J.S. Mainstone-Aus
Woomera	Australia	Australia	31.11 S	136.54 E	41.8 S	209.	B.J. Fraser-Aus
Godhavn	Greenland	Denmark	69.23 N	53.52 W	79.9 N	32.5	<div> <div>R.R. Heacock-US</div> <div>V.P. Hessler-US</div> <div>J.F. Kenney-US</div> <div>V.A. Troitskaya-USSR</div> <div>W.H. Campbell-US</div> </div>
Sukkertoppen	Greenland	Denmark	65.42 N	52.90 W	76.1 N	28.7	
Thule	Greenland	Denmark	76.61 N	68.65 W	88.9 N	357.8	
Witteveen	Netherlands	Netherlands	52.82 N	06.67 E	54.1 N	91.2	D.v. Sabben-N
Noord Oost Polder	Netherlands	Netherlands	52.72 N	05.65 E	51.4 N	90.	Utrecht Obs.-N
*Sodankyla	Finland	Finland	67.37 N	26.63 E	63.8 N	120.0	V.P. Hessler-US
*Nurmijarvi	Finland	Finland	60.52 N	24.65 E	57.9 N	112.6	"
*Ensooping	Sweden	Sweden	59.58 N	17.13 E	58.5 N	105.3	F. Elemen-Swe
*Kiruna	Sweden	Sweden	67.83 N	20.42 E	65.3 N	115.7	1-5
*Reykjavik (Leirvogur)	Iceland	U.S.	64.18 N	21.70 W			<div> <div>W.H. Campbell-US</div> <div>T. Nagata</div> </div>
Rude Skov	Denmark	Denmark	55.85 N	12.45 E	55.9 N	98.5	
Dourbes	Belgium	Belgium	50.1 N	04.6 E	52.0 N	87.7	
*Furstenfeldbruck	W. Germany	W. Germany	48.17 N	11.28 E	48.9 N	92.4	H. Voelker-Ger
*Wingst	W. Germany	W. Germany	53.73 N	09.73 E	54.5 N	94.	"
" Göttingen	W. Germany	W. Germany	51.53 N	09.95 E	52.3 N	93.8	"
*Nagyecsk	Hungary	Hungary	47.63 N	16.72 E	47.2 N	98.3	A. Adair-H E. Veró

* Standard observatories producing normal magnetograms.

OBSERVATORY	COUNTRY	SPONSOR	POSITION COORDINATES			PC FREQ. BAND	ANALYST
			GEOGRAPHIC	GEOMAGNETIC			
			LAT.	LONG.	LAT.	LONG.	
*Roburent	Italy	Italy	44.3 N	07.88 E	45.8 N	88.5	1-5 H. Voelker-Ger
*Toledo	Spain	Spain	39.88 N	04.05 W	43.9 N	74.7	
*Chambon-la-Forêt	France	France	48.02 N	02.27 E	50.5 N	84.4	{ F. Glangaud-Fr E. Selzer
*Hurouque	France	France	43.92 N	0.35 W	47.0 N	79.4	R. Schlich
Garchy	France	France	47.30 N	03.10 E	49.6 N	84.9	{ J. Roquet -Fr E. Selzer
*Lerwick, Shetland	Scotland	U.K.	60.13 N	01.18 W	62.5 N	88.6	W.F. Stuart-UK
Eskdalemuir, Dumfriesshire	Scotland	U.K.	55.32 N	03.20 W	58.5 N	82.9	"
Hartland	England	U.K.	51.00 N	04.48 W	54.6 N	79.0	"
Mt. St. Hilaire, Que.	Canada	Canada	45.53 N	73.15 W	57. N	355.	C.C. Ku-Can
Great Whale River	Canada	Canada	55.33 N	77.83 W	66.6 N	374.4	W. Campbell-US
Baie St. Paul, Que.	Canada	Canada	47.37 N	70.55 W	58.7 N	0.7 W	J.A. Jacobs-Can
Leduc (U of Alberta)	Canada	Canada	53.6 N	113.4 W	61.4 N	300.	{ J.A. Jacobs-Can G. Rostoker-Can
Red Deer, Alb.	Canada	Canada	52.3 N	113.8 W	60.3 N	300.	"
Ft. Reliance, NWT	Canada	Canada	62.7 N	109. W	71.4 N	300.	"
Cambridge Bay NWT	Canada	Canada	69.1 N	105. W	85. N	300.	"
Ft. Smith, NWT	Canada	Canada	60.0 N	111.9 W	68.5 N	300.	"
Ft. Chepewyan, Alb.	Canada	Canada	58.7 N	111. W	67.3 N	300.	"
McMurray, Alb.	Canada	Canada	56.7 N	111.3 W	65. N	300.	"
*Meenook, Alb.	Canada	Canada	54.62 N	113.33 W	61.8 N	301.	"
Calgary, Alb.	Canada	Canada	51.0 N	114.2 W	59. N	300.	"
*Victoria, B.C.	Canada	Canada	48.5 N	123.42 W	54.2 N	293.	B. Caner-Can
Bar I	Canada	Canada	69.6 N	140.18 W	70.4 N	258.1	R.R. Heacock-US

* Standard observatories producing normal magnetograms.

OBSERVATORY	COUNTRY	SPONSOR	GEOGRAPHIC		GEOMAGNETIC		Pc FREQ. BAND	ANALYST
			POSITION COORDINATES					
			LAT.	LONG.	LAT.	LONG.		
Inuvik, NWI	Canada	Canada	68. N	130. W	72. N	268.	1-5	R.R. Heacock-US
Borrego, Calif.	U.S.	U.S.	33.36 N	116.28 W				W.H. Campbell-US
Ft. Yukon, Alaska	U.S.	U.S.	66.57 N	145.25 W				"
Austin, Texas	U.S.	U.S.	30.18 N	97.47 W	40.0 N	326.	2-5	{ H.W. Smith-US F.X. Bostick-US
Ashland, Maine	U.S.	U.S.	46.3 N	68.3 W	57.0 N	3.	2-5	
LaGrande, Oregon	U.S.	U.S.	45.5 N	118. W	50.0 N	297.	2-5	
Lebanon, N.J.	U.S.	U.S.	39.63 N	74.5 W	50.0 N		2-5	T.J. Herron-US
Cougar Mt., Seattle, Wn.	U.S.	U.S.	47.63 N	122.35 W	52.15 N	293.	1-5	J.F. Kenney-US
Tulalip, Seattle, Wn.	U.S.	U.S.	48.08 N	122.19 W	53.6 N	292.	1-5	"
Fredericksburg, Va.	U.S.	U.S.	38.2 N	77.38 W	49.6 N	349.8	1-5	V. Lincoln-US
Tucson, Arizona	U.S.	U.S.	32.25 N	110.83 W	40.4 N	312.2		
Dallas, Texas	U.S.	U.S.	32.98 N	96.75 W	43.0 N	327.7	1-5	{ A.W. Green, Jr.-US A.A.J. Hoffman-US
Koror, Palau Is.	U.S.	U.S.	07.27 N	134.53 E	3.3 S	203.5	1-5	N. Matuura-Japan
Guam, Mariana Is.	U.S.	U.S.	13.45 N	144.75 E	4.0 N	212.9	1-5	"
Maui, Hawaii	U.S.	U.S.	20.71 N	156.26 W	21.1 N	266.5	1-5	W.H. Campbell-US
Dillingham AFB, Hawaii	U.S.	U.S.	21.6 N	158.0 W	21.0 N	270.	2-5	{ H.W. Smith-US F.X. Bostick-US

OBSERVATORY	COUNTRY	SPONSOR	POSITION COORDINATES				BAND	ANALYST
			GEOGRAPHIC		GEOMAGNETIC			
			LAT.	LONG.	LAT.	LONG.		
Boulder, Colo.	U.S.	U.S.	40.14 N	105.24 W	48.9 N	43.1	1-5	W. Campbell-US
Kingston, Rhode Island	U.S.	U.S.	41.62 N	71.73 W				"
Newport, Wash.	U.S.	U.S.	48.26 N	117.12 W			1-5	{ W.H. Campbell-US J.A. Jacobs-Can
College, Alaska	U.S.	U.S.	64.87 N	147.83 W	64.6 N	256.5	1-5	{ W. Campbell-US R.R. Heacock-US
Sitka, Alaska	U.S.	U.S.	57.07 N	135.33 W	60.0 N	275.3	1-5	R.R. Heacock-US
Anchorage, Alaska	U.S.	U.S.	61.10 N	149.55 W	60.9 N	258.1	1-5	"
Pt. Barrow, Alaska	U.S.	U.S.	71.30 N	156.75 W	68.5 N	241.1	1-5	"
Kotzebue, Alaska	U.S.	U.S.	66.92 N	162.60 W	63.7 N	242.1	1-5	{ J. Annexstad-US R.R. Heacock-US ³⁵
Standford, Calif.	U.S.	U.S.	37.26	122.10 W	43.5 N	299.0	1-3	A.O. Fraser-Smith-US
Centro Geofisico, Soroa	Cuba	Cuba	22.97 N	82.15 W	34.1 N	345.3		V.A. Troitskaya-USSR
Apia	Samoa Is.	W. Samoa	13.80 S	171.77 W	16.1 S	260.2	2-5	
Manila	Philippines	Philippines	14.7 N	121.1 E	06.0 N	182.	2-5	{ H.W. Smith-US F.X. Bostick-US

OBSERVATORY	COUNTRY	SPONSOR	POSITION COORDINATES			FREQ. BAND	ANALYST
			GEOMAGNETIC	LAT.	LONG.		
			LAT.	LONG.	LAT.	LONG.	
Baguio	Philippines	Philippines	16.42 N	120.6 E	05.1 N	189.2	F.N. Glover-Phil
Cebu	Philippines	Philippines	10.33 N	123.9 E	0.0	189.	"
Pamatai	Tahiti	France	17.57 S	149.57 W	15.35 S	77.23	R. Remiot
Nemambetsu	Japan	Japan	43.54 N	144.12 E	34.0 N	208.4	Y. Kato-Japan
Kanoya	Japan	Japan	31.25 N	130.53 E	20.5 N	198.1	T. Saito
Asa	Japan	Japan	32.53 N	131.01 E	22.0 N	198.1	T. Sakurai
Simosato	Japan	Japan	33.34 N	135.56 E	23.0 N	202.4	T. Hirasawa
Kakioka	Japan	Japan	36.14 N	140.11 E	26.0 N	206.0	K. Yanagihara
Onagawa	Japan	Japan	38.26 N	141.28 E	28.3 N	206.8	M. Kawamura
							S. Utashiro
Trinidad	B.W. Indies	U.S.	10.42 N	61.38 W	21.0 N	9.	H.W. Smith-US
Camp Toruquero	Puerto Rico	U.S.	18.29 N	66.25 W	30.0 N	5.	F.X. Bostick-US
Paramaribo	Surinam	Netherlands	05.82 N	55.22 W	16.9 N	15.3	D.V. Sabben-N
Huancayo	Peru	Peru	12.1 S	75.3 W	00.6 S	353.8	
Jicamarca	Peru	U.S.	11.95 S	76.87 W			W.H. Campbell-US
Eights	Antarctica	U.S.	75.23 S	77.17 W	63.9 S	355.3	W.H. Campbell-US
Byrd	Antarctica	U.S.	79.98 S	120.02 W	70.4 S	336.	"
Plateau	Antarctica	U.S.	79.47 S	40.58 E			"
South Pole	Antarctica	U.S.	90.00 S	0.0			"
McMurdo	Antarctica	U.S.	77.85 S	166.62 E			"

OBSERVATORY	COUNTRY	SPONSOR	POSITION COORDINATES			PC FREQ. BAND	ANALYST
			GEOGRAPHIC LAT.	LONG.	GEOMAGNETIC LAT.	LONG.	
Halley Bay	Antarctica	U.K.	75.52 S	26.7 W	65.8 S	24.3	D.M. Finlayson-UK
Mirny	Antarctica	USSR	66.55 S	93.02 E	77.0 S	146.8	V.A. Troitskaya-USSR
Novolazarevskaya	Antarctica	USSR	74.77 S	11.82 E	66.2 S	53.6	S.V. Burtakov-USSR
Syowa Bay	Antarctica	Japan	69.0 S	39.35 E	69.7 S	77.7	T. Nagata-Japan
*Wilkes	Antarctica	Australia	66.25 S	110.58 E	77.7 S	179.2	T. Oguti
*McQuarrie Island	Antarctica	Australia	54.5 S	158.95 E	61.6 S	243.1	J.A. Thomas-Aus
*Mawson	Antarctica	Australia	67.58 S	62.9 E	73.2 S	103.4	J.A. Thomas-Aus
Termination Point (Travis)	Antarctica	France	66.67 S	140.0 E	75.6 S	230.9	J. Annexstad-US
Vostok	Antarctica	USSR	78.45 S	106.87 E	89.2 S	92.6	W.H. Campbell-US
Base Roi Baudouin	Antarctica	Belgium-Netherlands	70.42 S	24.30 E			R.R. Heacock-US
LaRoche Codon Amsterdam	Indian Ocean	France	37.83 S	77.57 E	46.70 S	140.6	V.P. Hessler-US
Port Alfred Crozet	Indian Ocean	France	46.43 S	51.87 E	51.20 S	109.3	J.F. Kenney-US
*Kerguelen	Indian Ocean	USSR-France	49.35 S	70.20 E	56.5 S	127.8	V.A. Troitskaya-USSR
							R. Gendrin-Fr
							R. Schlich-Fr

* Standard observatories producing normal magnetograms.

OBSERVATORY	COUNTRY	SPONSOR	POSITION COORDINATES			Pc FREQ BAND	ANALYST
			GEOGRAPHIC LAT	LONG.	GEOMAGNETIC LAT.	LONG.	
*Resolute Bay	Canada	Canada	74.70 N	94.90 W	83.0 N	289.6	
*Baker Lake	Canada	Canada	64.33 N	96.03 W	73.8 N	315.2	
*Tromsø	Norway	Norway	69.67 N	18.97 E	67.1 N	116.7	
*Ottawa	Canada	Canada	45.2 N	75.5 W	57.0 N	351.5	
*Edinburgh	Scotland	Scotland	55.92 N	3.19 W	55.3 N	79.4	
*Niamey	German D.R.	German D.R.	52.07 N	12.68 E	52.2 N	96.6	
*Grocka	Yugoslavia	Yugoslavia	44.63 N	20.77 E	43.6 N	100.9	
*Zaria	Nigeria	Nigeria	11.15 N	7.65 E	13.7 N	79.1	
*Durban	R.S. Africa	R.S. Africa	29.92 S	30.93 E	31.5 S	93.0	

* Standard observatories producing normal magnetograms.

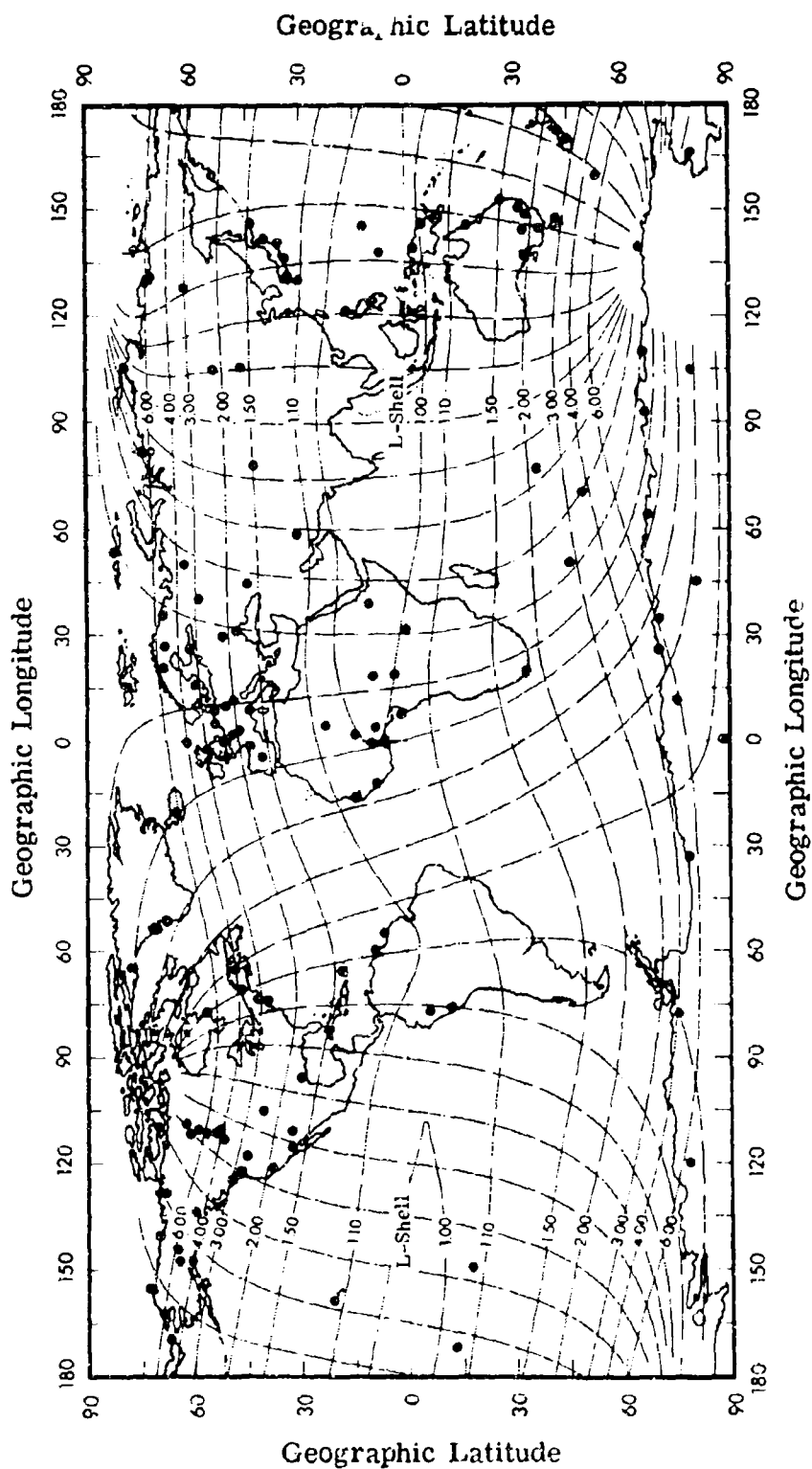


Fig. 5. Global distribution of rapid-run geomagnetic observatories. Geomagnetic coordinates, based on the Jensen and Cain model (1976 & 1977a), are field-line L-shells and longitude lines spaced at hour intervals.

TABLE 2. U. S. SPACECRAFT MAGNETOMETER EXPERIMENTS

VEHICLE	DATES	TRAJECTORY			INSTRUMENT	ENERGY RANGE	EXPERIMENTER
		PERIOD	INCLINATION	PERIGEE/ APOGEE			
Pioneer 1 (58 n 1)	10/58 -			113,137 km	search coil	1-2000 Y	C.P. Sonett
Explorer 6 (59 s 1)	8/59 -	12.7 hr	47°	250/4200 km	search coil	1-2000 Y	C.P. Sonett E.J. Smith D.L. Judge P.J. Coleman
Vanguard 3 (59 n 1)	9/59 -	130 min	33°	510/3750	proton pre- cession		J.P. Heppner
Pioneer 5 (60 a 1)	3/60 -	311.64 days	3.35°	.806/.993 Au	search coil	1-2000 Y	C.P. Sonett 40 D.L. Judge P.J. Coleman
Explorer 10 (61 n 1)	3/61 -	112 hr	33°	161/233000 km	rubidium v. 2 fluxgates		J.P. Heppner T.L. Skillman C.S. Scearce N.F. Ness
Explorer 12 (61 v 1) Mariner 2	8/61 - 12/61 8/62 - 12/62	26.5 hr	33°	300/77300 km	fluxgate triaxial fluxgate	0-100 Y	L. Cahill C.P. Sonett P.J. Coleman L. Davis E.J. Smith
Explorer 14	10/62 - 6/63	36 hr	33°	300/100000 km	triaxial fluxgate		L. Cahill
Thor-Able-Star (63-38C)	9/63 -	107.3 min	89.9°	1072/1135 km	3-axis		A.J. Zmuda
Explorer 18 (63-64A)	11/63 -	93.5 hr	33.3°	192/196960 km	rubidium v. 2 fluxgates	± 40 Y ± 1/4 Y	N.F. Ness

VEHICLE	DATES	TRAJECTORY			INSTRUMENT	ENERGY RANGE	EXPERIMENTER
		PERIOD	INCLINATION	PERIGEE/ APOGEE			
Vela 2B (64-40B)	7/64 -	100.0 hr	39.1°	74490/131530km	search coil		E.W. Greenstadt
OGO 1 (64-54A)	9/64 -	64.3 hr	57.4°	34723/115059km	search coil		E.J. Smith
Explorer 21 (64-60A)	10/64 -	26.5 hr	33.5°	300/77300 km	fluxgate	± 1000 Y	N.F. Ness D.H. Fairfield
(64-83C)	12/64 - 6/65	106.2 min	89.992°	1040/1089 km	rubidium v.	15,000 - 31,000 Y	A.J. Zmuda F.T. Heuring W. Radford
Explorer 26	12/64 - 10/66	7 hr	33°	300/30000 km	dualaxis fluxgate		L. Cahill
OGO 2 (65-81A)	10/65 -	104.3 min	87.4°	418/1514 km	rubidium v.	1 Y	J.C. Cain J.P. Heppner
	10/65 - 10/67				search coil		E.J. Smith
Pioneer 6 (65-105A)	12/65 -			.814/.985 AU	fluxgate		N.F. Ness
OGO 3 (66-49A)	6/66 -	48.5 hr	62.5°	6274/116078km	search coil		E.J. Smith
					rubidium v. fluxgates	0.1-700 Y	J.P. Heppner
Explorer 33 (66-52A)	6/66 -	14-34 days	30-40°	643/4727 - 140000/1,50000 km	triaxial fluxgate	0-64 Y	N.F. Ness K.W. Behannon
					"	0-200 Y	C.P. Sonett
Pioneer 7 (66-75A)	8/66 -			1.010/1.125 AU	fluxgate	0-32 Y	N.F. Ness F.W. Mariani
ATS-1 (66-110A)	12/66 -	23.9 hr	0.9°	35779/35794 km	2 fluxgates		P.J. Coleman

VEHICLE	DATES	TRAJECTORY			INSTRUMENT	ENERGY RANGE	EXPERIMENTER
		PERIOD	INCLINATION	PERIGEE/ APOGEE			
Vela 4A (67-40A)	4/67	111.1 hr	33.7°	108355/1114071 km	search coil		E.W. Greenstadt
Explorer 34 (67-51A)	5/67	103.6 hr	71.3°	3618/207581 km	triaxial fluxgate	0-32 Y 0-128 Y	N.F. Ness D.H. Fairfield
Dodge (67-66F)	7/67	22 hr	7°	40,000 km nearly circular	triaxial fluxgate	0.2-250 Y	A.J. Zmuda M. Dwarkin W. Radford
Explorer 35 (67-70A)	7/67	selenocentric orbit			fluxgate	0-2000 Y	C.P. Sonett
OGO 4 (67-73A)	7/67	11.5 hr	156°	800/7650 km	triaxial fluxgate "	0-24 Y 0-200 Y	N.F. Ness K.W. Behannon C.P. Sonett
Pioneer 8 (67-123A)	12/67	97.0 min	86.0°	409/831 km	fluxgate rubidium v.	0-64 Y	J.P. Heppner
(68-02A)	1/68	112.2 min	74°	1.0/1.1 AU	single fluxgate	0-32 Y 0-96 Y	N.F. Ness F. Mariani S. Cantarano
OGO 5 (68-14A)	3/68	63.3 hr	31.1°	1078/1580 km	uniaxial fluxgate	± 500 Y	A.J. Zmuda J.C. Armstrong
Pioneer 9 (68-100A)	11/68			271/148186 km	triaxial fluxgate		P.J. Coleman
					rubidium v.		J.P. Heppner
				0.7/1.0 AU	triaxial fluxgate	0-200 Y	C.P. Sonett

VEHICLE	DATES	TRAJECTORY			INSTRUMENT	ENERGY RANGE	EXPERIMENTER
		PERIOD	INCLINATION	PERIGEE/ APOGEE			
OGO 6	6/69 -	99.6 min	81.9°	400/1087	triaxial search coil		E.J. Smith
IMP G	6/69 -	3.4 days	86.8°	400+/ 176717 km	triaxial fluxgate		N.F. Ness D.H. Fairfield
S ³ A	69	Future			triaxial magnetometer		L. Cahill
IMP I	70	"			triaxial magnetometer		N.F. Ness
AIMP H	71	"			triaxial magnetometer		N.F. Ness
AIMP J	72	"			triaxial magnetometer		N.F. Ness

REFERENCES

1. Jacobs, J. A. and T. Watanabe (1965), Micropulsations of the earth's electromagnetic field in the frequency range 0.1-10 c/s, in *Progress in Radio Science 1960-1963, Vol. IV*, pp. 67-84, Elsevier, Amsterdam.
2. Hultqvist, B. (1966), Plasma waves in the frequency range 0.001-10 cps in the earth's magnetosphere and ionosphere, *Space Sci. Rev.*, 5, 599-695.
3. Campbell, W. H. (1966), A review of the equatorial studies of rapid fluctuations in the earth's magnetic field, *Ann. Geophys.*, 22, 492-501.
4. Campbell, W. H. (1967), Geomagnetic pulsations, in *Physics of Geomagnetic Phenomena*, pp. 821-909, Academic Press, New York.
5. Campbell, W. H. (1968), Rapid geomagnetic field variations observed at conjugate locations, *Radio Science*, 3, 726-739.
6. Gendrin, R. (1967), Structure, polarisation et propagation des oscillations hydromagnetiques, *Ann. Geophys.*, 23, 153-170.
7. Troitskaya, V. A., and A. V. Gul'elmi (1967), Geomagnetic micropulsations and diagnostics of the magnetosphere, *Space Sci. Rev.*, 7, 689-768.
8. Saito, T. (1969), Geomagnetic pulsations, *Space Sci. Rev.*, 9, in press.
9. Heppner, J. P. (1967), Recent measurements of the magnetic field in the outer magnetosphere and boundary regions, *Space Sci. Rev.*, 7, 166-190.
10. Frandsen, A. M. A., R. E. Holzer, and E. J. Smith, (1969), OGO search coil magnetometer experiments, *IEEE Trans. Geoscience Electronics*, GE-7, in press.

11. Alfvén, H. and C. G. Fälthammer (1963), *Cosmical Electrodynamics*, Clarendon, Oxford.
12. Thompson, W. B. (1962), *An Introduction to Plasma Physics*, Pergamon, Oxford.
13. Stix, T. H. (1962), *The Theory of Plasma Waves*, McGraw-Hill, New York.
14. Booker, H. G. and R. B. Dyce (1965), Dispersion of waves in a cold magnetoplasma from hydromagnetic to whistler frequencies, *Radio Science*, 69A, 463-492.
15. Sugiura, M. (1965), Propagation of hydromagnetic waves in the magnetosphere, *Radio Science*, 69D, 1133-1147.
16. Seshadri, S. R. (1965), The magnetoionic theory at hydromagnetic frequencies, *J. Atmospheric Terrest. Phys.*, 27, 617-631.
17. Dowden, R. L. (1965), "Micropulsation mode" propagation in the magnetosphere, *Planet. Space Sci.*, 13, 761-772.
18. Fejer, J. A. and K. F. Lee (1967), Guided propagation of Alfvén waves in the magnetosphere, *J. Plasma Physics*, 1, 387-406.
19. Hayakawa, M., J. Ohtsu, and A. Iwai (1969), Ducted propagation of hydromagnetic whistlers in the magnetosphere, *Proc. Res. Inst. Atmospheric Nagoya University*, 16, 91-100.
20. Akasofu, S. I. (1965), Attenuation of hydromagnetic waves in the ionosphere, *Radio Science*, 69D, 361-366.
21. Field, E. C. and C. Greifinger (1965), Transmission of geomagnetic micropulsations through the ionosphere and lower exosphere, *J. Geophys. Res.*, 70, 4885-4899.
22. Dessler, A. J. (1965), The dissipation of hydromagnetic wave energy in the ionosphere, in *Space Research V*, pp. 119-124, North-Holland, Amsterdam.
23. Sorenson, W. R. (1968), Investigation of possible ionospheric heating by hydromagnetic waves, *J. Geophys. Res.*, 73, 287-294.

24. Tepley, L. and R. K. Landshoff (1966), Waveguide theory for ionospheric propagation of hydromagnetic emission, *J. Geophys. Res.*, 71, 1499-1504.
25. Manchester, R. N. (1966), Propagation of pc 1 micropulsations from high to low latitudes, *J. Geophys. Res.*, 71, 3749-3754.
26. Altman, C. and E. Fijalkow (1968), Mechanism of transmission of hydromagnetic waves through the earth's lower ionosphere, *Nature*, 220, 53-55.
27. Altman, C. and E. Fijalkow (1969), The mechanism of hydromagnetic wave propagation through the lower ionosphere, *J. Geophys. Res.*, in press.
28. Greifinger, C. and P. S. Greifinger (1968), Theory of hydromagnetic propagation in the ionospheric waveguide, *J. Geophys. Res.*, 73, 7473-7490.
29. Gendrin, R. (1965), Gyroresonance radiation produced by proton and electron beams in different regions of the magnetosphere, *J. Geophys. Res.*, 70, 5369-5383.
30. Watanabe, T. (1966), Quasi-linear theory of transverse plasma instabilities with applications to hydromagnetic emissions from the magnetosphere, *Can. J. Phys.*, 44, 815-835.
31. Jacobs, J. A. and T. Watanabe (1966), Amplification of hydromagnetic waves in the magnetosphere by a cyclotron instability process with applications to the theory of hydromagnetic whistlers, *J. Atmospheric Terrest. Phys.*, 28, 235-253.
32. Cornwall, J. M. (1966), Micropulsations and the outer radiation zone, *J. Geophys. Res.*, 71, 2185-2199.
33. Gendrin, R. (1967), Mécanismes D'interaction, *Ann. Geophys.*, 23, 313-332.

34. Liemohn, H. B. (1967), Cyclotron-resonance amplification of VLF and ULF whistlers, *J. Geophys. Res.*, 72, 39-55.
35. Kennel, C. F. and H. V. Wong (1967a), Resonant particle instabilities in a uniform magnetic field, *J. Plasma Phys.*, 1, 75-80.
36. Kennel, C. F. and H. V. Wong (1967b), Resonantly unstable off-angle hydromagnetic waves, *J. Plasma Phys.*, 1, 81-104.
37. Cocke, W. B. and Cornwall, J. M. (1967), Theoretical simulation of micropulsations, *J. Geophys. Res.*, 69, 2843-2856.
38. Gul'elmi, A. V. (1968), Cyclotron instability of outer radiation-belt protons, *Geomag. Aeron.*, 8, 331-336.
39. Criswell, D. R. (1969), Pc 1 Micropulsation activity and magnetospheric amplification of 0.2 - to 5.0-Hz hydromagnetic waves, *J. Geophys. Res.*, 74, 205-224.
40. Liemohn, H. B. (1969), The cyclotron resonance amplification of whistlers in the magnetosphere, in *Proc. NATO institute on plasma waves*, ed. J. O. Thomas, in press.
41. Bird, H. H. and G. Schmidt (1969), Transverse wave propagation and instabilities within the magnetosphere, *J. Geophys. Res.*, 74, 3993-4002.
42. Kennel, C. F. and H. Petschek (1966), Limit on stably trapped particle fluxes, *J. Geophys. Res.*, 71, 1-28.
43. Trakhtengerts, V. Yu. (1966), Stationary states of the earth's outer radiation zone, *Geomag. Aeron.*, VI, 638-645.
44. Trakhtengerts, V. Yu. (1967), Nonlinear theory of the cyclotron instability of the radiation belts of the earth, *Geomag. Aeron.*, VII, 269-271.
45. Gendrin, R. (1968), Pitch angle diffusion of low energy protons due to gyroresonant interaction with hydromagnetic waves, *J. Atmospheric Terrest. Phys.*, 30, 1313-1330.

46. Hasegawa, A. (1969), Heating of the magnetospheric plasma by electromagnetic waves generated in the magnetosheath, *J. Geophys. Res.*, 74, 1763-1771.
47. Hollweg, J. V. (1969), Stochastic heating of protons by fast hydromagnetic wave, *J. Geophys. Res.*, 74, 2899-2907.
48. Southwood, D. J., J. W. Dungey, and R. J. Etherington (1968), Neglected plasma instability involving bounce resonance, *Nature*, 219, 56-57.
49. Roberts, C. S. and M. Schultz (1968), Bounce resonant scattering of particles trapped in the earth's magnetic field, *J. Geophys. Res.*, 73, 7361.
50. Roberts, C. S. (1969), Pitch angle diffusion of electrons in the magnetosphere, *Rev. Geophys.*, 7, 305-337.
51. Siscoe, G. L., L. Davis, Jr., E. J. Smith, P. J. Coleman, and D. E. Jones (1967), Magnetic fluctuations in the magnetosheath: mariner 4, *J. Geophys. Res.*, 72, 1-17.
52. Heppner, J. P., M. Sugiura, T. L. Skillman, B. G. Ledley, and M. Campbell (1967), OGA-A magnetic field observations, *J. Geophys. Res.*, 72, 5417-5471.
53. Smith, E. J., R. E. Holzer, M. G. McLeod, and C. T. Christopher, (1967), Magnetic noise in the magnetosheath in the frequency range 3-300 hz, *J. Geophys. Res.*, 72, 4803-4813.
54. Behannon, K. W. (1968), Mapping of the earth's bow shock and magnetic tail by explorer 33, *J. Geophys. Res.*, 73, 907.
55. Cummings, W. D. and P. J. Coleman, Jr. (1968), Magnetic fields in the magnetopause and vicinity at synchronous altitude, *J. Geophys. Res.*, 73, 5699-5718.
56. Smith, E. J., R. E. Holzer, and C. T. Russell (1969), Magnetic emissions in the magnetosheath at frequencies near 100 hz, *J. Geophys. Res.*, 74, 3027-3036.

57. Olson, J. V., R. E. Holzer, and E. J. Smith (1969) High frequency magnetic fluctuations associated with the earth's bow shock, *J. Geophys. Res.*, 74, 4601-4617.
58. Russell, C. T. and R. E. Holzer (1969), OGO 3 observations of ELF noise in the magnetosphere, *J. Geophys. Res.*, 74, 755-777.
59. Russell, C. T., R. E. Holzer, and E. J. Smith (1969), OGO 3 observations of ELF noise in the magnetosphere. Part 2 the nature of the equatorial noise, *J. Geophys. Res.*, in press.
60. Jacobs, J. A. and T. Watanabe (1964), Micropulsation whistlers, *J. Atmospheric Terrest. Phys.*, 26, 825-829.
61. Obayashi, T. (1965) Hydromagnetic whistlers, *J. Geophys. Res.*, 70, 1069-1078.
62. Gendrin, R. E. and V. A. Troitskaya (1965), Preliminary results of a micropulsation experiment at conjugate points, *Radio Science*, 69D, 1107-1116.
63. Kenney, J. F. and H. B. Knafllich (1967), A systematic study of structured micropulsations, *J. Geophys. Res.*, 72, 2857-2869.
64. Campbell, W. H. (1967), Low attenuation of hydromagnetic waves in the ionosphere and implied characteristics in the magnetosphere for Pc 1 events, *J. Geophys. Res.*, 72, 3429-3445.
65. Baranski, L. N., L. A. Geller, and B. N. Kasak (1967), Propagation velocity of Pc 1 type micropulsation "pearls" of the earth electromagnetic field, *Rpts. Acad. Sci. USSR*, 177, 85-88.
66. Troitskaya, V. A., L. N. Baranski, P. A. Vinogradov, A. V. Sobolev, and S. I. Solov'yev (1968), Some properties of the Pc 1 type of pulsations of the earth's electromagnetic field observed simultaneously over a large area (Russia), *Geomag. Aeron.*, 8, 726-730.

67. Annexstad, J. O. and C. I. Wilson (1968), Pc 1 fine structure phase shift at high-latitude conjugate points, *J. Geophys. Res.*, 73, 3063-3065.
68. Glangeaud, F., J. Roquet, and E. Selzer (1968), Microstructures à diverses latitudes et composition spectrale des perturbations magnétiques de février 1965 et mars 1966, *Ann. Geophys.*, 24, 871-877.
69. Manchester, R. N. (1968), Correlation of Pc 1 micropulsations at spaced stations, *J. Geophys. Res.*, 73, 3549-3556.
70. Heacock, R. R. (1968), Large amplitude Pc 1 events at college, *J. Geomag. Geoelec.*, 20, 263-269.
71. Bagnall, F. T. (1969), The direction of arrival of Pc 1 micropulsations, in *Proc. of Sympos. on Geomagnetic Micropulsations*, ed. B. J. Fraser, University of Newcastle, Newcastle NSW.
72. McPherron, R. L., G. K. Parks, F. V. Coroniti, and S. H. Ward (1968), Studies of the magnetospheric substorm 2. Correlated magnetic micropulsations and electron precipitation occurring during auroral substorms, *J. Geophys. Res.*, 73, 1697-1713.
73. Wilhelm, K. (1968), Occurrences of Pc 1 pulsations in the course of magnetospheric substorms, *J. Geophys. Res.*, 73, 7491-7501.
74. Plyasova-Bakunina, T. A. and E. T. Matveyeva (1968), Relationships between pulsations of the Pc 1 type and magnetic storms, *Geomag. Aeron.*, 8, 153-155.
75. Matveyeva, E. T., M. N. Gnevyshev, and V. A. Troitskaya (1968), Relationship between 11-year cyclic variations in pulsations of the pearl type (Pc 1) and solar activity, *Geomag. Aeron.*, 8, 783-786.
76. Tepley, L. R. (1966), Recent investigations of hydromagnetic emission Part I. Experimental observations, *J. Geomag. Geoelec.*, 8, 227-256.
77. Wentworth, R. C. (1966), Recent investigations of hydromagnetic emissions Part II. Theoretical interpretation, *J. Geomag. Geoelect.*, 18, 257-273.
78. Watanabe, T. (1965), Determination of the electron distribution in the magnetosphere using hydromagnetic whistlers, *J. Geophys. Res.*, 70, 5839-5848.

79. Dowden, R. L. and M. W. Emery (1965), The use of micropulsation "whistlers" in the study of the outer magnetosphere, *Planet. Space Sci.*, 13, 773-779.
80. Dowden, R. L. (1966), Micropulsation "nose whistlers" a helium explanation, *Planet. Space Sci.*, 14, 1273
81. Liemohn, H. B., J. F. Kenney, and H. B. Knafllich (1967), Proton densities in the magnetosphere from pearl dispersion measurements, *Earth Planetary Sci. Letters*, 2, 360-366.
82. Kenney, J. F., H. B. Knafllich, and H. B. Liemohn (1968), Magnetospheric parameters determined from structured micropulsations, *J. Geophys. Res.*, 73, 6737-6749.
83. Troitskaya, V. A., E. T. Matveyeva, K. G. Ivanov, and A. V. Gul' elmi (1968), Change in the frequency of Pc 1 micropulsations during a sudden deformation of the magnetosphere, *Geomag. Aeron.*, 8, 784-786.
84. Fraser, B. J. (1968), Temporal variations in Pc 1 geomagnetic micropulsations, *Planet. Space Sci.*, 16, 111-124.
85. Taylor, H. A., Jr., H. C. Brinton, and M. W. Pharo, III (1968), Contraction of the plasmasphere during geomagnetically disturbed periods, *J. Geophys. Res.*, 73, 961-968.
86. Kenney, J. F., H. B. Knafllich, and H. A. Taylor, Jr. (1969), Private communication comparing ground and satellite observations.
87. Gendrin, R., S. Lacourly, M. Gokhberg, O. Malevskaya, and V. A. Troitskaya (1966), Polarisation des oscillations hydro-magnetiques de type Pc 1 observées en deux stations geomagnetiquement conjuguées, *Ann Geophys.*, 22, 329-337.
88. Heacock, R. R. and V. P. Hessler. (1967), Polarization characteristics of Pc 1 micropulsations at college, *Planet. Space Sci.*, 15, 1361-1374.

89. Roquet, J. (1969), Sur un cas particulier de pulsations géomagnétiques observées dans les régions équatoriales d' Afrique, *C. R. Acad. Sc. Paris*, 268, 581-584.
90. Summers, W. R. (1969), Polarization of Pc 1 micropulsations at middle latitudes, in *Proc. of Sympos. on Geomagnetic Micropulsations*, ed. B. J. Fraser, University of Newcastle, Newcastle, NSW.
91. Kenney, J. F., H. B. Knafllich, and H. B. Liemohn (1967), Measurement and interpretation of ULF and VLF power spectra, in *Proc. Conjugate Point Sympt., Boulder, Colorado, June 1967*, IERTM-ITSA 72, 2, III-11-1-III-12-25.
92. Kenney, J. F., T. K. Deaton, and J. E. Miller (1967), Improved displays for measuring power spectra of complex nonstationary signals, *Rev. Sci. Instr.*, 38, 665-667.
93. Campbell, W. H. and E. C. Stiltner (1965), Some characteristics of geomagnetic pulsations at frequencies near 1 c/s, *Radio Science*, 69D, 1117
94. Gendrin, R. E., S. Lacourly, V. A. Troitskaya, M. Gokhberg, and R. V. Shepetnov (1967), Caracteristiques des pulsations irregulieres de periode decroissante (I.P.D.P.) et leurs relations avec les variations du flux des particules piegees dans la magnetosphere, *Planet. Space Sci.*, 15, 1239-1259.
95. Bakhur, L. V., V. B. Lyatskiy, and V. P. Selivanov (1967), Relationship between pp and variations of auroral luminescence, *Geomag. Aeron.*, 7, 164-166.
96. Troitskaya, V. A. and N. F. Mal'tseva (1967), Possible influence of ionospheric conditions on the formation of pulsation intervals of decreasing period in the electromagnetic field of the earth, *Geomag. Aeron.*, 7, 915-916.
97. Knafllich, H. B. and J. F. Kenney (1967), IPDP events and their generation in the magnetosphere, *Earth Planetary Sci. Letters*, 2, 453-459.

98. Troitskaya, R. V. Shchepetnov, and A. V. Gul'eimi (1968),
Evaluation of electric fields in the magnetosphere according
to frequency drift of hydromagnetic emissions (Russian),
Geomag. Aeron., 8, 794
99. Gendrin, R. and S. Lacourly (1968), Irregular micropulsations
and their relations with the far magnetospheric perturbations,
Ann. Geophys., 24, 1-7.
100. Inter-Union Commission on Solar Terrestrial Physics (1968),
STP Notes No. 1, IUCSTP Secretariat c/o National Academy
of Sciences, Washington, D. C.
101. Inter-Union Commission on Solar Terrestrial Physics (1968),
STP Notes No. 2, IUCSTP Secretariat c/o National Academy
of Sciences, Washington, D. C.
102. Inter-Union Commission on Solar Terrestrial Physics (1969),
STP Notes No. 3, IUCSTP Secretariat c/o National Academy
of Sciences, Washington, D. C.
103. Inter-Union Commission on Solar Terrestrial Physics (1969),
STP Notes No. 4, IUCSTP Secretariat c/o National Academy
of Sciences, Washington, D. C.
104. Space Science Board (1968), *Physics of the Earth in Space;
A Program of Research: 1968-1975*, National Academy of
Sciences, Washington, D.C.
105. Space Science Board (1969), *Physics of the Earth in Space;
The Role of Ground-based Research*, National Academy of
Sciences, Washington, D.C.
106. World Data Center A (1969), *Geomagnetism*, Environmental Sciences
Services Administration, Rockville, Md.
107. Dudziak, W. F., D. D. Kleineche, T. J. Kostigen (1963),
Graphic displays of geomagnetic geometry, *General Electric
Rpt. RM 63TMP-2 and DASA 1372*.

ADDITIONAL REFERENCES

- 6a. Gendrin, R. (1967), Progrés récents dans l'étude des ondes T.B.F. et E.B.F., *Space Sci. Rev.*, 7, 314-395.
- 30a. Roux, A. and P. Frey (1969), Non-linear frequency shift in hydromagnetic and whistler modes, *Canad. J. Phys.*, in press.
- 38a. Feigin, F. Z. and V. L. Iakimenko (1968), Generation and amplification of "pearls" by means of a cyclotronic plasma instability in the inner proton zone, in *Fifth Soviet Winter School for Cosmic Physics*, edited by the Polar Geophysical Institute, Moscow, pp. 254-257.
- 68a. Glangeaud, F. (1969), Conditions suivant lesquelles peut être définie la notion d'un parcours au sol pour certaines pulsations du champ magnétique terrestre, *Compte-Rendus*, 268, 113-116.
- 7a. Troitskaya, V. A. (1967), Micropulsations and the state of the magnetosphere, in *Solar-Terrestrial Physics*, edited by J. W. King and W. S. Newman, Academic Press, New York, 213-274.
- 16a. Dawson, J. A. (1966), Hydromagnetic wave propagation near 1 c/s in the upper atmosphere and the properties and interpretation of Pc 1 micropulsations, *NBS Tech. Note* 342.
- 31a. Dobes, K. (1968), The character of cyclotron instability of hydromagnetic waves, *Czech. J. Phys.*, B18, 1133-1141.
- 62a. Schlich, M. R. (1966), Sur une propriété des micropulsations du type pc, et pi, observées en points magnétiquement conjugués de moyenne latitude, *C. R. Acad. Sc. Paris*, 262, 1742-1745.
- 65a. Schlich, R., and J. Bitterly (1967), Variations magnétiques rapides enregistrées en des stations proches, *Ann. Geophys.*, 23, 407-412.
- 106a. World Data Center A (1969), *Catalogue of Data on Solar-Terrestrial Physics*, National Academy of Sciences, Washington, D.C.
- 107a. Jensen, D. C., and J. C. Cain (1962), An interim geomagnetic field (abstract), *J. Geophys. Res.*, 67, 3568-3569.